THE JOURNAL OF BIOLOGICAL CHEMISTRY
Vol. 273, No. 21, Issue of May 22, pp. 12870–12880, 1998

Printed in U.S.A.

Conservative Mutations in the Immunosuppressive Region of the Bovine Leukemia Virus Transmembrane Protein Affect Fusion but Not Infectivity *in Vivo**

(Received for publication, July 10, 1997, and in revised form, March 16, 1998)

Jean-Stéphane Gatot‡, Isabelle Callebaut§, Jean-Paul Mornon§, Daniel Portetelle, Arsène Burny, Pierre Kerkhofs¶, Richard Kettmann‖, and Luc Willems**

From the Unité de Biologie Moléculaire, Faculté Universitaire des Sciences Agronomiques, Avenue Maréchal Juin 13, B5030 Gembloux, Belgium, the ¶Institut National de Recherches Vétérinaires, Groeselenberg 99, B1180 Uccle, Belgium, and the §Equipe Systèmes Moléculaires et Biologie Structurale, LMCP, CNRS UMR7590, Université P6, Case 115, 4 Place Jussieu, F75252 Paris, France

Many retroviruses, including bovine leukemia virus (BLV), contain a highly conserved region located about 40 amino acids downstream from the fusion peptide within the sequence of the external domain of the transmembrane (TM) protein. This region is notably thought to be involved in the presentation of the NH_2-terminal peptide to allow cell fusion. By using hydrophobic cluster analysis and by analogy with the influenza A hemagglutinin structures, the core of the TM structure including this particular region was predicted to consist, in the BLV and other retroviral envelope proteins, of an α-helix followed by a loop region, both docked against a subsequent α-helix that forms a triple-stranded coiled coil. The loop region could undergo, as in hemagglutinin, a major refolding into an α-helix integrating the coiled coil structure and putting the fusion peptide to one tip of the molecule. Based on this model, we have identified amino acids that may be essential to the BLV TM structure, and a series of mutations were introduced in the BLV *env* gene of an infectious molecular clone. A first series of mutations was designed to disturb the coiled coil structure (substitutions with proline residues), whereas others would maintain the general TM structure. When expressed by Semliki Forest virus recombinants, all the mutated envelope proteins were stable and efficiently synthesized in baby hamster kidney cells. Both proline-substituted and conservative mutants were strongly affected in their capacity to fuse to CC81 indicator cells. In addition, it appeared that the integrity of the TM coiled coil structure is essential for envelope protein multimerization, as analyzed by metrizamide gradient centrifugation. Finally, to gain insight into the role of this coiled coil in the infectious potential of BLV *in vivo*, the mutated TM genes were introduced in an infectious and pathogenic molecular clone and injected into sheep. It appeared that only the conservative mutations (A60V and A64S) allowed maintenance of viral infectivity *in vivo*. Since these mutations destroyed the ability to induce syncytia, we conclude that efficient fusion capacity of the recombinant envelopes is not a prerequisite for the infectious potential of BLV *in vivo*. Viral propagation of these mutants was strongly affected in some of the infected sheep. However, the proviral loads within half of the infected animals (2 out of 2 for A60V and 1 out of 4 for A64S) were close to the wild-type levels. In these sheep, it thus appears that the A60V and A64S mutants propagate efficiently despite being unable to induce syncytia in cell culture.

The infectivity of enveloped viruses is thought to be mediated by surface glycoproteins that are responsible for the recognition of the target cell and for the fusion of both viral and cellular membranes (1). The envelope proteins of the retroviruses are composed of the following two subunits: the extracellular (SU)[1] protein that binds to the receptor and the transmembrane (TM) glycoprotein that anchors the envelope complex into the cell membrane. Both subunits are first synthesized as a single glycosylated polypeptide that is subsequently cleaved into the mature SU and TM proteins. In the case of bovine leukemia virus (BLV), the envelope gene is first translated as a 72-kDa precursor product (see Refs. 2 and 3 for review). This glycoprotein is then cleaved by a cellular protease into two mature products, an SU protein of 51 kDa (gp51) and a TM protein of 30 kDa (gp30). Both the gp51 and gp30 subunits are required for viral infectivity since deletions within the *env* gene do not yield replication-competent virus *in vivo* (4). Since the *env* gene sequence is highly conserved among different strains, it has been generally assumed that the BLV envelope is the result of high molecular constraints that appeared during evolution (5). Altogether these observations assign a key role for the envelope gene in the biological properties of the BLV virus.

Previous work has devoted a series of functions to this BLV gp30 protein. In addition to the TM domain of the TM protein, two other regions are involved in essential mechanisms mediated by the envelope protein. First, a hydrophobic peptide located at the amino-terminal end is essential for virus-medi-

* This work was supported by the Association Belge Contre le Cancer, the Association Sportive Contre le Cancer, the Bekales Foundation, the Caisse Générale d'Epargne et de Retraite, the Fonds National de la Recherche Scientifique, the Sidaction, and the Service de Programmation pour la Politique Scientifique Grant SSTC P4/30. The costs of publication of this article were defrayed in part by the payment of page charges. This article must therefore be hereby marked "*advertisement*" in accordance with 18 U.S.C. Section 1734 solely to indicate this fact.

‡ Télévie Fellow of the Fonds National de la Recherche Scientifique.
‖ Directeur de Recherches of the Fonds National de la Recherche Scientifique.
** Maître de Recherches of the Fonds National de la Recherche Scientifique. To whom correspondence should be addressed. Tel.: 32-81-622157; Fax: 32-81-613888; E-mail: willems.l@fsagx.ac.be.

[1] The abbreviations used are: SU, extracellular; TM, transmembrane; BLV, bovine leukemia virus; ELISA, enzyme-linked immunosorbent assay; PCR, polymerase chain reaction; WT, wild type; HA, hemagglutinin; gp, glycoprotein; MoMuLV, Moloney murine leukemia virus; HCA, hydrophobic cluster analysis; BHK, baby hamster kidney; PBS, phosphate-buffered saline; HTLV, human T-cell lymphotrophic virus; ITAM, immunoreceptor tyrosine based activation motif; HIV-1, human immunodeficiency virus type 1.

ated cell fusion. This so-called fusion peptide destabilizes the cellular membrane probably through an oblique insertion within the lipid bilayer (6, 7). Fusion peptides are particularly rich in small amino acids such as alanine and glycine which could play a key role in their conformational mobility, helping them to destabilize lipid bilayers (8). A second domain located in the cytoplasmic tail of the BLV TM protein appears to exert an essential role in signal transduction. Indeed, its carboxyl-terminal extremity contains two Y*XX*L sequences that share similarities with immunoreceptor tyrosine-based activation motifs or ITAM (9, 10). These motifs are able to transduce signals through the cell membrane when they are fused to the CD8 molecule and triggered by an anti-CD8 monoclonal antibody (11, 12). These ITAM sequences appear to be required for viral replication *in vivo* since their mutation affects either infectivity or efficient propagation in the sheep animal model (13). Another region of the BLV TM protein, located about 40 amino acids downstream from the fusion peptide, is also of interest because it shares strong similarities with the immunosuppressive CKS17 peptide that has been shown to inhibit the proliferation of lymphocytes in culture (14). This peptide is present in a wide variety of retroviral envelope proteins and exhibits similar immunosuppressive functions in different systems (15–17).

At the beginning of this study, the only available three-dimensional model of an envelope glycoprotein that mediates fusion was the hemagglutinin protein (HA) of the influenza A virus (18). Like retroviral envelopes, HA is proteotically processed in a receptor-binding subunit (HA1) and a membrane-spanning subunit (HA2) that contains at its NH_2 terminus a fusion peptide. The HA complex is organized as a trimer of HA1 in interaction with HA2. In its latent form (designated BHA), the trimeric HA2 chains are major components of a mainly α-helical stem domain (19, 20). From amino to carboxyl termini, HA2 is composed of an α-helix (A) located next to the fusion peptide followed by a loop region (B), both being docked against a long helix (C and D) forming in the trimeric structure a triple-stranded α-helical coiled coil (Fig. 1, *left*). At the low pH of endosomes, a major structural change occurs at both ends of the HA2 chain giving rise to a structure called TBHA (21) (Fig. 1, *right*). The loop region, which was maintained in a non-helical conformation as a result of extensive interactions with HA1, is reorganized into an α-helix incorporating the coiled coil structure and inducing the ejection of the fusion peptide over a distance of at least 150 Å in a "spring-loaded" manner. This refolding of the loop into a helix is thought to be involved in the presentation of the NH_2-terminal peptide to allow cell fusion with the target cell membrane. Another conformational change is also observed in the middle of the coiled coil structure where seven residues refold to form a bend allowing the helix D and three short β-strands to "jack-knife" back and pack against helix C.

Despite striking functional similarities, HA2 and retroviral TM proteins share very low levels of sequence identity (far below the so-called "twilight" level of 25–30%) and are not alignable with classical methods (22). However, regions having high helical propensity and 4–3 heptad repeats characteristic of coiled coil structures have been observed in retroviral TM proteins like in HA2 (23–25), suggesting a common general scaffold for all the fusogenic TM proteins including a trimeric organization (26). These predictions were further supported by the recent experimental trimeric structure of a peptide corresponding to the amino-terminal extremity of Moloney murine leukemia virus (MoMuLV) TM protein (27), as well as very recently by those of two interacting peptides of the human immunodeficiency virus type 1 (HIV-1) TM protein (28, 29).

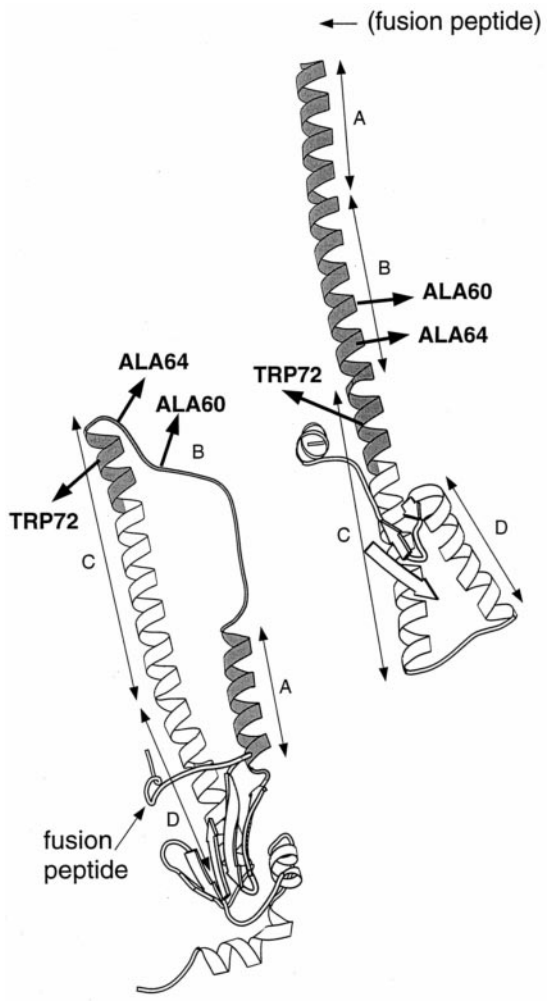

FIG. 1. **The HA2 conformational change from a latent form (BHA, *left*) to a fusogenic form (TBHA2, *right*).** Only monomers are represented to allow comprehension. Both structures are trimers interacting through the central helix C (incorporating A and B in the fusogenic form) forming the core of the coiled coil. Two major changes are observed as follows: *loop B* is refolded into an α-helix while seven residues in the middle of helix *C–D* unfold, reversing the chain direction of helix D. The apolar fusion peptide, which was removed in the fusogenic form to allow solubilization, moves to one tip of the molecule. Comparison of HA2 and retroviral TM sequences have led us to decipher a similar region between these fusogenic viruses (*shaded*) that would constitute the common coiled coil core of the fusogenic forms (*boxed* in Fig. 2). The corresponding positions of three of the mutations that were introduced in the BLV gp30 TM protein and that are located in the common coiled coil defined in Fig. 2 are indicated with *arrows*, according to our modeling.

Both structures are strikingly similar to that of the fusogenic TBHA2 structure (29). As no direct experimental structure of latent forms of retroviral TM protein has yet been determined, it remains to be proven that retroviral TM proteins also use a spring-loaded mechanism with SU proteins acting as clamps that hold the NH_2-terminal regions of TM proteins in a non-coiled coil conformation. Since retrovirus-induced cell fusion is pH-independent, another dynamic must explain the process of refolding, perhaps with the help of additional viral or cellular factor(s) (1).

Based on the BHA and TBHA2 structures as well as on multiple alignments of retroviral TM proteins, a model of the BLV gp30 was constructed. In order to assess further the importance of this structure in the biological properties of the BLV, a series of mutations were introduced in the BLV TM protein, and their effects were analyzed *in vitro* by metrizamide

centrifugation and in cells for syncytia induction. We have chosen to work on the BLV TM protein because this system also allows the final evaluation of the behavior of recombinant proviruses *in vivo*.

EXPERIMENTAL PROCEDURES

Hydrophobic Cluster Analysis—Alignment of the retroviral and hemagglutinin TM proteins was performed using the hydrophobic cluster analysis (HCA) method (22, 30, 31). In contrast to other methods that work only on the maximization of sequence similarities, HCA is based on the analysis of hydrophobic amino acid clusters throughout the molecules. Indeed, hydrophobic amino acids are not distributed randomly along the protein sequences but are grouped into clusters that represent the internal faces of regular secondary structures (32). Successive correspondences of hydrophobic clusters along a structural domain are the signature of similar three-dimensional folding patterns. In related proteins, a precise alignment can then be deduced by proceeding outward from the hydrophobic clusters to linker regions where gaps are allowed. Three-dimensional manipulations were performed with the MANOSK program (33), run on an Evans and Sutherland terminal PS390. Crystallographic data were taken from the Protein Data Bank (34).

Construction of the Recombinant Proviruses—Plasmids pBLVIX (which contains the wild-type virus pBLV344), pBLVY186D, pBLVY197D, pBLVY(186 + 197)D, and pBLVS1L + A4L (previously called pBLV6073, pBLV6106, pBLV6073 + 6106, and pBLVCV1, respectively) were described elsewhere (4, 13). To construct the other recombinant proviruses, mutations were introduced into the *env* sequence cloned into plasmid pCMVenv that contains the envelope gene of the wild-type 344 provirus (13). These mutations were performed by site-directed mutagenesis using a two-step PCR procedure essentially as described previously (4). Therefore, the following sense (S) and complementary (C) oligonucleotides that contain the selected mutations were used as follows: 5695S (5′-GCTTAATGTGCCCTCTGTGGTC-3′), 5695C (5′-GACCACAGAGGGCACATTAAGC-3′), Val5695S (5′-GCTTAATGTGGTCTCTGTGGTC-3′), Val5695CPlus (5′-CGGTTCTGGGCGACCACAGAGACCACATTAAGC-3′), 5707S (5′-CTCTGTGGTCCCCCAGAACCGA-3′), 5707C (5′-TCGGTTCTGGGGGACCACAGAG-3′), Ser5707S (5′-CTCTGTGGTCTCCCAGAACCGA-3′), Ser5707CPlus (5′-CTAGCCCCCGTCGGTTCTGGGAGACCACAGAG-3′), 5731S (5′-GGGGCTAGATTTGTTGTACATC-3′), 5731C (5′-GATGTACAACAAATCTAGCCCC-3′), 5764S (5′-TCAAAGCCTAGCTCCCACGATC-3′), and 5764C (5′-GATCGTGGGAGCTAGGCTTTGA-3′).

A first round of PCR reactions allowed the amplification of two fragments encompassing the *env* gene as follows: a 5′-end insert (using the T7 primer and one of the complementary oligonucleotides) and a 3′-end fragment (using the SP6 primer and the corresponding sense oligonucleotide). After PCR, the two inserts were migrated on an agarose gel, purified using the Sephaglas Bandprep kit (Amersham Pharmacia Biotech), and amplified in a second round of PCR using the SP6 and T7 oligonucleotides. The resulting DNAs that contain the entire *env* gene sequence were then digested with the *Hin*dIII and *Xba*I restriction endonucleases and introduced into the corresponding sites of the pGem7 plasmid (Promega). In order to verify the presence of the desired substitution and the absence of *Taq* DNA polymerase errors, the mutated fragments were then sequenced by the dideoxy chain termination procedure using a set of primers located along the *env* gene (T7 sequencing kit, Amersham Pharmacia Biotech). After their verification, the mutated *env* sequences were cloned in the *Nco*I-*Xba*I sites of plasmid pBLVIX to generate pBLVA60P, -A60V, -A64P, -A64S, -W72L, and -C83A. Restriction analysis and nucleotide sequencing were performed to verify the integrity of the resulting constructs. These plasmids were then purified by centrifugation on cesium chloride gradient as described by Sambrook (35).

Construction of the pSFVenv Recombinant Vectors—To express the envelope proteins in the Semliki Forest virus system, the recombinant envelope genes were first cloned into the pSFV3 vector (36). To locate the *env* initiation codon next to the promoter, about 270 nucleotides had to be eliminated upstream from the 5′-end of the envelope gene. Therefore, the wild-type envelope gene was PCR-amplified with an oligonucleotide that contains a *Bam*HI restriction site (5′-AAAATGGATCCCAAAGAACGACGGTCCCG-3′, sense, 3′-position 4637 according to Ref. 37) and the oligonucleotide DREX4 (5′-CCCCAACCAACAACACTTGCTT-3′, antisense, 3′-position 7039 according to Ref. 37). The PCR amplification product was then digested by the *Bam*HI restriction endonuclease and inserted in the corresponding site of the pSFV3 vector, yielding plasmid pSFVenvWT. To construct the plasmids that express the mutated envelopes (pSFVenvA60P, pSFVenvA60V, pSFVenvA64P, pSFVenvA64S, pSFVenvW72L, pSFVenvC83A, pSFVenvY186D, pSFVenvY197D, and pSFVenvY(186 + 197)D), the *Nco*I-*Bam*HI *env* fragments (at positions 4925–6997 following the numeration of Rice *et al.* (37)) were isolated from the recombinant proviruses and inserted in the corresponding sites of pSFVenvWT. To construct pSFVenvWTa and pSFVenvS1L + A4L, the 2072-base pair *Nco*I-*Sma*I *env* fragment of the pSFVenvWT vector (at positions 4925 and in the plasmid linker) was replaced by an *Nco*I-*Pvu*II insert from plasmids pBLVS1L + A4L or pSP64-ENV (6).

Expression of the Recombinant BLV Envelopes into BHK Cells—General procedures about the Semliki Forest virus expression system were described elsewhere (36). In brief, pSFV3 plasmids containing the wild-type or recombinant envelope genes were linearized with the *Spe*I restriction endonuclease and used as templates for *in vitro* transcription. The RNAs were synthesized at 37 °C for 1 h in 50-μl reaction mixtures containing 1.5 μg of linearized plasmid, 40 mM Tris-HCl (pH 7.5), 6 mM $MgCl_2$, 2 mM spermidine, 10 mM NaCl, 5 mM dithiothreitol, 1 mM each ATP, CTP, and UTP, 500 μM GTP, 30 units of SP6 RNA polymerase, 60 units of RNasin (Promega), and 1 mM $m^7G(5')ppp(5')G$ (Amersham Pharmacia Biotech). The efficiency of transcription was evaluated by migration of a 2-μl aliquot on a 1% agarose gel. After precipitation with isopropyl alcohol, equal amounts of RNA were resuspended in 20 μl of ice-cold TE buffer (10 mM Tris-HCl, 1 mM EDTA (pH 7.5)) and electroporated into baby hamster kidney (BHK) cells. Therefore, BHK cells were trypsinized, washed with phosphate-buffered saline (PBS, 137 mM NaCl, 2.7 mM KCl, 4.3 mM NaH_2PO_4, 1.47 mM KH_2PO_4 (pH 7.4)), and resuspended at 10^7 cells per ml in ice-cold PBS. The purified RNAs were then electroporated into four million BHK cells by two consecutive pulses (830 V, 40 microfarads, maximum resistance) using a Cellject electroporation system (Eurogentec). After transfection, the cells were immediately diluted in 15 ml of G-minimum Eagle's medium (Life Technologies, Inc.) complemented with 10% heat-inactivated serum and cultivated at 37 °C for 48–60 h.

Syncytia Formation Assay—To visualize the multinucleated cells, we used a colorimetric assay based on the use of β-galactosidase protein. Therefore, RNAs were transcribed *in vitro* from plasmid pSFVLacZ that expresses the *lacZ* gene (36). These RNAs were mixed with the transcripts from each wild-type and mutant pSFVenv plasmids at a 1 to 4 ratio and transfected into 5×10^5 BHK cells. After electroporation, the BHK cells were cultivated in G-minimum Eagle's medium for 4 h to allow their attachment to the dishes. Then they were co-cultivated for 20 h with 2 million CC81 indicator cells to evaluate their fusion capacity. After culture, the cells were washed with PBS and fixed for 10 min at 4 °C in PBS containing 2% formaldehyde and 0.2% glutaraldehyde. After an additional wash with PBS, the β-galactosidase activity was revealed by incubation of the cells in the presence of a reaction mixture containing 1 mg per ml of 4-chloro-5-bromo-3-indolyl-β-galactopyranoside, 5 mM potassium ferrocyanide, 5 mM potassium ferricyanide, and 2 mM $MgCl_2$ in PBS. Syncytia containing more than four nuclei were counted under the light microscope in 10 different fields at a 10-fold magnification.

Metrizamide Gradient Centrifugation—The wild-type and recombinant envelope proteins were expressed by the Semliki Forest virus expression system in BHK cells. After 48 h of culture, the cells were harvested and lysed by freezing them once at −80 °C. The cell lysates were then layered on a linear 5–40% gradient of metrizamide (Sigma) in TNE (10 mM Tris-HCl, 150 mM NaCl, 1 mM EDTA (pH 8.3)) and centrifuged overnight at 4 °C in a TH641 rotor (Sorvall) at 13,000 rpm. Eighteen 600-μl fractions were collected from the gradient, and the proteins were precipitated by the addition of 300 μl of polyethylene glycol (PEG 8000) 30% (w/v), 0.4 M NaCl. After centrifugation, the proteins were resuspended in PBS, migrated onto a 12.5% polyacrylamide-sodium dodecyl sulfate gel, and analyzed by Western blot to reveal the presence of gp51 and gp30. The Western blot procedures were performed essentially as described by the manufacturer (Boehringer Mannheim chemiluminescence Western blotting kit) using a serum from a BLV-infected sheep (sheep 38) and an anti-bovine immunoglobulin monoclonal antibody (4G7) coupled to peroxidase.

In Vivo Infection and Semi-quantitative PCR—The recombinant pBLV plasmids were transfected into sheep as described previously (38). In short, sheep were injected intradermally with 100 μg of plasmid DNA mixed with 200 μg of *N*-(1-(2,3-dioleoyloxy)propyl)-*N,N,N*-trimethylammonium methylsulfate (Boehringer Mannheim) in 1 ml of Hepes-buffered saline (20 mM Hepes, 150 mM NaCl (pH 7.4)). The sheep were maintained under controlled conditions at the National Institute for Veterinary Research (Uccle, Belgium), where natural transmission between sheep has never been observed. Sera were collected weekly and

analyzed for BLV sero-positivity by immunodiffusion and indirect gp51 ELISA (39).

To evaluate the proviral loads, blood samples (500 μl) were mixed with an equal volume of freshly prepared lysis buffer (0.32 M sucrose, 10 mM Tris-HCl (pH 7.5), 5 mM $MgCl_2$, 1% Triton X-100). The samples were centrifuged for 20 s, and the pellets were resuspended in 1 ml of lysis buffer by vortexing. This step was repeated twice. The samples were then resuspended in 500 μl of PCR buffer (10 mM Tris-HCl, 1.5 mM $MgCl_2$, 50 mM KCl (pH 8.3)) and incubated with 6 μl of proteinase K (5 mg/ml) for 1 h at 50 °C. Five-microliter aliquots were amplified by PCR in the presence of 200 μM each deoxynucleotide triphosphate, 200 ng of primers, and 1 unit of *Taq* DNA polymerase (Boehringer Mannheim). The two oligonucleotides used were PCRTB (5′-CGGGGCGGTGGCGGCGCCTAGG-3′ at position 8000 according to the numeration of Rice *et al.* (37)) and PCRTD (5′-TAACGACAAAATTATTTCTTGTC-3′ at position 7012). The reaction mixtures were overlaid with 75 μl of mineral oil, denatured for 5 min at 94 °C, and amplified by 25 cycles of PCR (30 s at 94 °C, 30 s at 57 °C, and 1 min at 72 °C). After PCR, the samples were analyzed by Southern blot hybridization using a BLV Tax probe.

To ensure that the viruses that propagated *in vivo* were not revertants, the envelope sequences were amplified by nested PCR using four oligonucleotides: PCREA 5′-TCCTGGCTACTAACCCCCCCGT-3′ (position 4560); DREX4 5′-CCCCAACCAACAACACTTGCTT-3′ (position 7060); 5107S 5′-AATATGGGGAGATGATCCCCT-3′ (position 5097); and 5764C. The *env* genes were then directly sequenced with the 5609 primer 5′-CACCTCCCTGATCCACGTTC-3′ (position 5610) using the double-stranded DNA Cycle Sequencing system (Life Technologies, Inc.).

RESULTS

Modeling of the BLV gp30—To gain insight into the structure of the BLV gp30, we adopted a strategy based on the similarities shared by retroviral TM proteins, including the BLV gp30, with the influenza A hemagglutinin HA2 that was the only fusogenic TM protein whose three-dimensional structure was known at that time. However, because of the low level of sequence identity shared by the retroviral and influenza A virus TM proteins (below 20%), we used the HCA method (hydrophobic cluster analysis) to assess the putative structural similarities between these proteins and to perform their alignments. HCA is indeed a sensitive method of sequence analysis that is able to detect three-dimensional similarities between protein domains showing very limited relatedness. Its sensitivity at low levels of sequence identity, typically below the twilight zone (25–30%), stems from its ability to detect secondary structure elements (32). The effectiveness of the HCA method has been widely demonstrated (for review see Ref. 22).

The procedure of alignment of HA2 and BLV gp30 is helped by the consideration of all retrovirus sequences as exemplified in Fig. 2. Successive correspondences of hydrophobic clusters along the HA and retroviral TM proteins (*shaded* on the lower half of the plots, Fig. 2) indicated that both molecules might share a similar global three-dimensional folding pattern. In particular, the NH_2-terminal regions of retroviral TM proteins, located just after the fusion peptides, share striking similarities with the region including the helix A, loop B, and the first part of the helix C of the latent HA2 structure (the common coiled coil core, *boxed* in Fig. 2). In addition, the conservation of core residues positions a and d (essential to the maintenance of the trimeric coiled coil interactions; *white letters* on a *black background* on the upper half of the HCA plots, Fig. 2) further reinforces the alignment between HA2 and retroviral TM proteins including the BLV gp30. Moreover, β-branched residues such as isoleucine or valine at both the BLV corresponding amino acids of the HA2 a and d positions are also in favor of a trimeric organization instead of another geometry (40). The region following the first part of helix C, however, appears different in retroviral TM proteins. Indeed, it contains proline, glycine, and cysteine residues that are not observed in this position in HA2, suggesting that a structure different from the coiled coil conformation could exist in this region in retroviral TM proteins. The loop ending the coiled coil structure could therefore be located in retroviral TM proteins upstream relative to its position in HA2. As a consequence, region C, which represents the invariant coiled coil structure (in the latent as well as in the fusogenic form), could be shortened. This prediction has been strengthened by the structure of the fusogenic MoMuLV TM protein (Fig. 2). It remains now to be determined whether this particular region also adopts a different structure in the latent form, by analogy with the second major structural rearrangement observed during the HA2 fusogenic transition, or if this structure exists in both the fusogenic and latent forms.

On the basis of these similarities between the HCA patterns, we postulated a trimeric organization for the BLV gp30. Three-dimensional models of the BLV gp30 structure in its potential latent form as well as in its fusogenic form were elaborated on the basis of the alignments deduced from HCA (Fig. 2) and using the hemagglutinin experimental structures (BHA and TBHA2) as templates. Our attention was drawn by amino acids that could play a role in the fusion process. In this respect, the loop-helix region B is of particular interest. Especially in this region two alanines (Ala-60 and Ala-64), although not corresponding to critical positions a or d of the coiled coil structure, could be important for the conformational transition as alanine is known to be favored in α-helices. By contrast, other amino acids that are particularly conserved among oncoviral TM proteins and that share strong similarities with the CKS17 immunosuppressive peptide are located in the conformationally invariant region C (notably in the case of Trp-72). Finally, the region including three cysteines (Cys-83, Cys-90, and Cys-91) is also of interest as it has apparently no direct counterpart in HA2 (Fig. 2). It would not make part of the coiled coil in the fusogenic conformation as suggested by the structure of the MoMuLV TM peptide (Fig. 2). It is possible that this region adopts another conformation in the latent form, as suggested by the HA2 analogy.

Construction and Expression of Transmembrane Protein Mutants—Our model of the BLV TM protein reveals that the immunosuppressive region could be required for the dynamics of the fusion process. In particular, we predict that residues Ala-60 and Ala-64 are located in a loop in the latent form that is reorganized in an α-helix to allow fusion. To assess further the biological relevance of this model, we adopted a strategy based on the analysis of the functional activity of mutated TM proteins. Two series of mutations were considered as follows: those qualified as non-conservative, which are predicted to disturb the α-helix structure, and others designed to maintain the general theoretical structure of the protein. The non-conservative mutations were performed at positions 60 and 64 by introducing proline residues instead of alanines (Fig. 3). Proline residues are indeed known to be poorly represented in α-helices mainly as they cannot form stabilizing H^+ bonds along the main chain. To design the conservative equivalents in the same amino acids, alanines 60 and 64 were substituted with a valine or a serine residue, respectively. Based on HCA similarities, these two amino acids are indeed encountered, respectively, in the HIV-1 and hemagglutinin TM proteins and would maintain the integrity of the α-helix. In addition to these mutations within the immunosuppressive region, we also substituted residue 72 that is a tryptophan in BLV gp30 but a leucine in the TM protein from all other oncoviruses, including HTLV-I gp21. To investigate the importance of residue 72, we designed a mutant that contains a leucine instead of a tryptophan (Fig. 3).

These mutations within the immunosuppressive region were compared with substitutions in other domains of the TM pro-

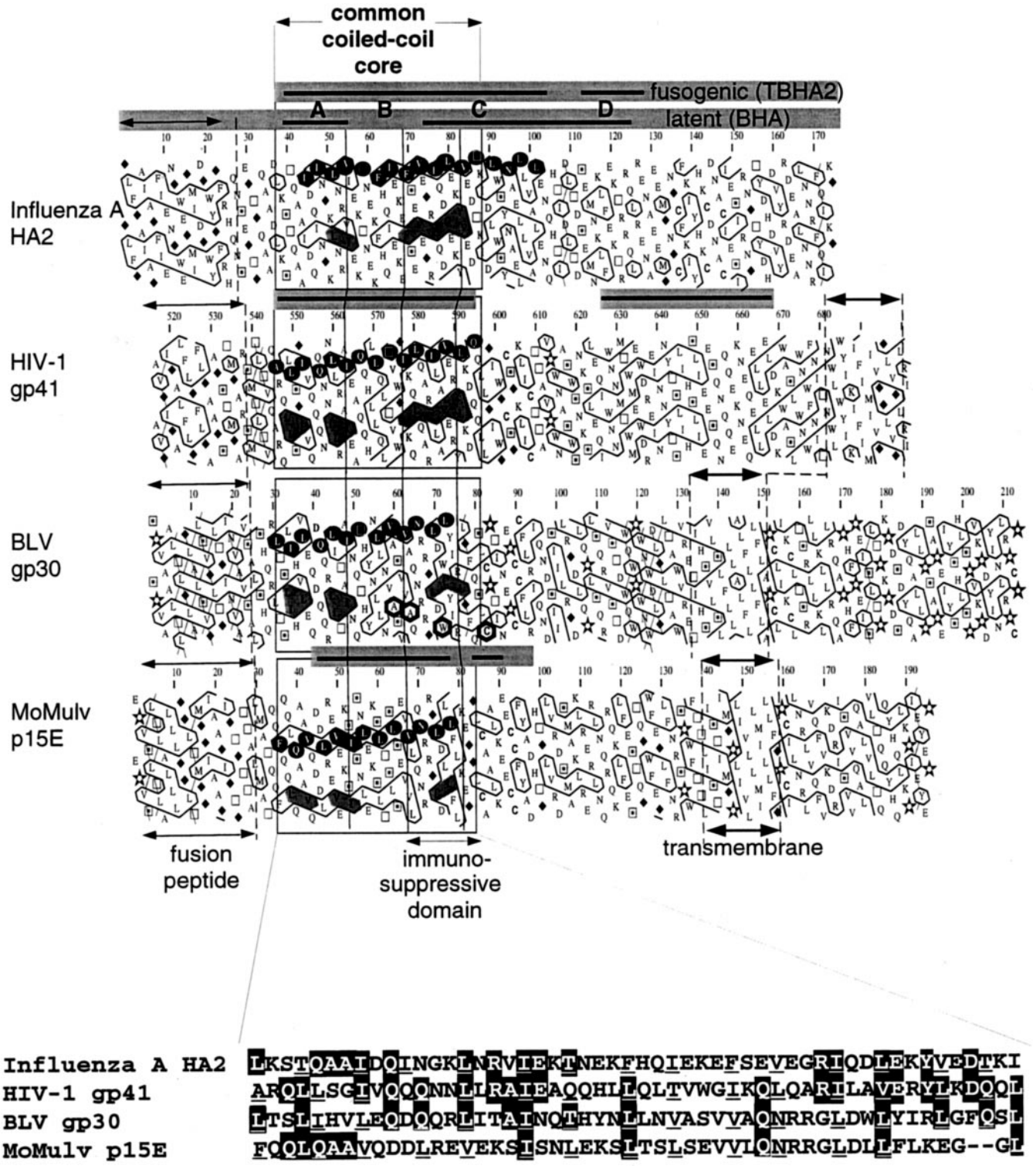

FIG. 2. **HCA comparison of the HA2 (Swissprot: hema_iaaic), HIV-1 gp41 (Swissprot: env_hv1br), BLV gp30 (Swissprot: env_blvj), and MoMuLV p15E (Swissprot: env_mlvmo) sequences.** Sequences are shown on a duplicated α-helical net with amino acid *numbers* indicated *above*. The hydrophobic residues are automatically contoured. They form clusters that mainly correspond to the inner faces of regular secondary structures (32). Four symbols are used regarding the specific structural behavior of the amino acids they represent: a *star* for proline, a *diamond* for glycine, a *square* for threonine, and a *square with a dot inside* for serine. The positions of the fusion peptides and the transmembrane segments are indicated by *arrows*, as well as the positions of the helical segments (*black strips*) when experimentally determined (HA2, see Refs. 19 and 21; HIV-1, see Ref. 29 encompassing the structure described by Ref. 28; MoMuLV, see Ref. 27) within the protein fragment under investigation (*shaded strips*). *Letters* above the HA2 structures correspond to those of Fig. 1. Note that the structures of the HIV-1 and MoMuLV TM proteins correspond only to fragments of the ectodomains and are thought to represent the fusogenic forms. Similar horizontal clusters (*shaded* on the *lower half* of the plots), typical of coiled coil structures, are found in the NH_2-terminal regions of the TM proteins (*boxed*). However, the coiled coil seems to be shortened in HIV-1 and especially in oncoviral TM proteins relative to HA2 (*A*, *B*, and *C* regions). This observation was later supported by the experimental structure of a fragment of the MoMuLV p15E. The successive a and d positions of the heptad repeats, as determined experimentally or predicted (for the BLV gp30 and the NH_2 terminus of the MoMuLV p15E (Phe-36, Gln-40, and Val-43)), are shown with *white letters* on a *black background* (*upper half* of the plots). The four mutated positions are *heavily circled*. Ala-60 and Ala-64 belong to the BLV putative B region that would be refolded in the conformational change, in contrast to Trp-72 that would be included on the invariant coiled coil. Cys-83

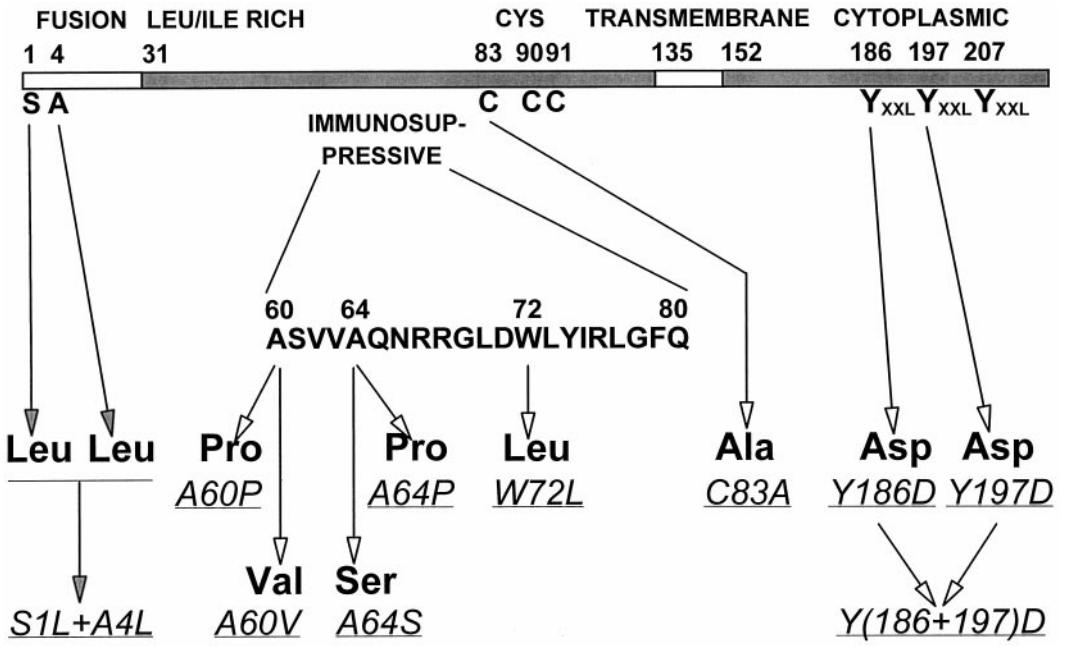

FIG. 3. **Schematic representation of the BLV transmembrane mutants.** The BLV gp30 protein has two hydrophobic regions (*open boxes*) as follows: the fusion peptide that is involved in fusion by oblique insertion into the cell membrane, and the transmembrane region that anchors the envelope complex in the membrane of the infected cells and in the virions. The immunosuppressive region is located between the end of a Leu/Ile-rich region (also called leucine zipper or heptad repeat) and the Cys region (also called immunodominant region). The cytoplasmic domain harbors three Y*XX*L motifs (also called ITAM) involved in intracellular signal transduction. A series of 10 mutations were introduced in the gene encoding the BLV gp30 protein: *S1L+A4L* (Ser-1 → Leu + Ala-4 → Leu), *A60P* (Ala-60 → Pro), *A60V* (Ala-60 → Val), *A64P* (Ala-64 → Pro), *A64S* (Ala-64 → Ser), *W72L* (Trp-72 → Leu), *C83A* (Cys-83 → Ala), *Y186D* (Tyr-186 → Asp), *Y197D* (Tyr-197 → Asp), and Y(186+197)D.

tein. The cysteines following the immunosuppressive region could play a role either in intra-chain disulfide bonding or in binding the SU protein. To possibly interfere with these structural constraints, we designed another mutant where cysteine 83 was replaced by an alanine (Fig. 3). The structure of a part of the MoMuLV TM ectodomain, obtained with a synthetic peptide, has revealed later that this cysteine probably would bind Cys-90, although no definite conclusion can be drawn for the moment only from a substructure of the TM protein, especially in the absence of the SU subunit. To design a reliable control in our syncytia formation experiments, we considered a mutant within the fusion peptide. As demonstrated previously, the dual substitution of both serine 1 and alanine 4 into leucine residues would completely disorganize the oblique orientation of the fusion peptide and in fact yields a TM mutant that is unable to form syncytia (6). Finally, we also included in our experiments a series of TM recombinants mutated in the ITAM motifs (*Y186D*, *Y197D*, and *Y(186+197)D*, Fig. 3). Only one of these mutations (Y186D) located in the cytoplasmic domain was shown to be compatible with infectivity *in vivo* (13).

All these different mutations were introduced in the TM gene from an infectious and pathogenic BLV provirus (38). To analyze their functional activities in cell culture, the recombinant envelopes were first cloned in the Semliki Forest virus expression vector and expressed in baby hamster kidney (BHK) cells. To compare the expression levels of the mutated TM proteins, the cell lysates were analyzed by Western blotting using the serum from a BLV-infected sheep. In this assay, it appeared that the external gp51 protein was expressed at similar levels among two different wild-type (WT and WTa) and the 10 mutated envelopes (Fig. 4*B*). Because of its poor immunogenicity, the gp30 glycoprotein could only be observed after over-exposition of the filter (Fig. 4*A*). By immunostaining, a 30-kDa protein was specifically revealed in all the lysates except one which contained the Y(186+197)D envelope mutant. In this latter case, the migration of the gp30 protein was slightly delayed, probably because of the mutation of two tyrosine residues that are putative targets for phosphorylation. Alternatively, it is possible that the gp30 protein might migrate aberrantly with different amino acid substitutions. In addition to this retarded form, the Y(186+197)D mutant also expressed the 30-kDa polypeptide. The specificity of these TM gene products was further supported by the absence of a 30-kDa protein in the negative control, *i.e.* a BHK lysate containing the β-galactosidase (LacZ, Fig. 4). From these Western blot experiments, we can also conclude that the mutations involved did not interfere with the processing of the envelope precursor polypeptide. To ensure that the envelopes were expressed at similar levels, the external gp51 glycoprotein was titrated by indirect enzyme-linked immunosorbent assay (39). This procedure, based on the immunodetection of gp51 with a panel of monoclonal antibodies, further supported the equal levels of envelope expression in the BHK lysates (data not shown). This assay was slightly modified to assess for the presence of the F, G, and H neutralizing epitopes on the external gp51 molecule. Therefore, only one monoclonal antibody at a time instead of a mix was used for detection. It appeared that the neutralizing epitope pattern (F+, G−, and H+) was conserved among all the mutated and wild-type envelope proteins (data not shown).

Mutations within the Immunosuppressive Region Affect Cell

is predicted to be linked to Cys-90 in a mainly non-helical region, but uncertainties remain about its conformation in the latent form. The proposed linear sequence alignment of the common coiled coil core of these four TM proteins as deduced from HCA is shown at the *bottom* with the a and d positions of the heptad repeat *underlined*. Identities are shown *white* on a *black background*. In this respect, the coiled coil structure of HA2 and retroviral TM proteins are alignable from their NH_2 terminus. Note that the TBHA2 structure contains two regions with an irregular 3–4-4–3 pattern of core residues, whereas the 4–3 periodicity is preserved throughout the length of the coiled coil of HIV-1 gp41 and MoMuLV p15E. Consequently, the TBHA2 coiled coil has a greater pitch than the retroviral ones.

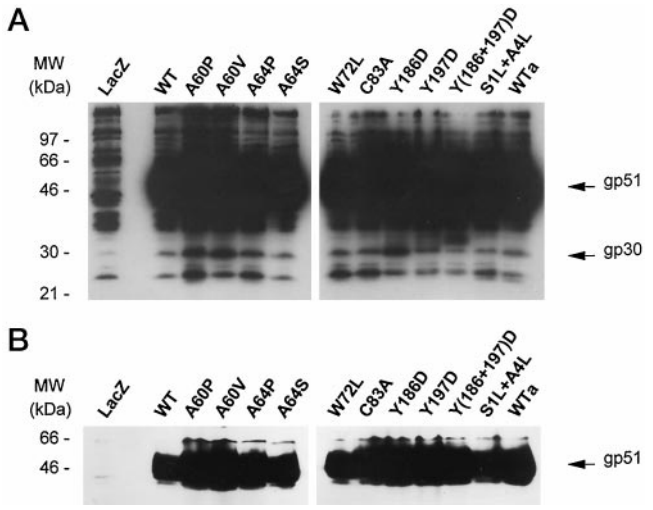

FIG. 4. **Expression of BLV wild-type and mutant envelope glycoproteins using the Semliki Forest virus expression system.** The wild-type (WT and WTa) and mutated (A60P, A60V, A64P, A64S, W72L, C83A, Y186D, Y197D, Y186D,Y197D (*Y(186+197)D*), and S1L + A4L) envelope genes were cloned into the pSFV expression vector (pSFVenv plasmids). WTa corresponds to the American strain of a wild-type BLV virus. After *in vitro* transcription, the corresponding purified RNAs were transfected into BHK cells by electroporation. As a control, the cells were also transfected with a pSFV expression vector encoding the *lacZ* gene. After cultivation during 60 h, the cells were harvested, and the corresponding cell lysates were migrated on an SDS-polyacrylamide gel. After electroblotting onto a nitrocellulose membrane, the proteins were subsequently incubated in the presence of the serum of sheep 38 and a secondary conjugate coupled to peroxidase. The presence of the gp51 and gp30 proteins was visualized by chemiluminescent detection (*A*, overexposed blot; *B*, blot exposed for 25 s).

Fusion—In addition to its role in anchoring the envelope complex, the TM protein is also involved in cell fusion. An essential region at the amino-terminal end of gp30, called the fusion peptide, is thought to destabilize the cell membrane by its oblique orientation within the lipid bilayer. Our model predicts that the immunosuppressive region is essential to the dynamics required for the presentation of this fusion peptide and its insertion within the target membrane. To validate this prediction, we next analyzed the fusogenic capacities of the different mutants. The experimental protocol is based on the co-cultivation of BHK cells that express the envelope proteins with CC81 indicator cells that are highly susceptible to fusion. When both kind of cells make contact, the envelope molecules inserted into the BHK membrane bind to the CC81 lipid bilayers and induce syncytia (large multinucleated cells). To facilitate the counting of the syncytia, the β-galactosidase protein was co-expressed together with the different envelopes. As positive controls, two wild-type envelope proteins from different viral strains (WT and WTa) efficiently induced the formation of syncytia (between 45 and 69 syncytia in ten 10-fold magnification fields). These numbers were arbitrarily normalized to the levels of the wild-type (WT) envelope, settled to 100% (Fig. 5).

As a negative control, the S1L + A4L mutant that was previously shown to be deficient for cell fusion only yielded background levels of syncytia. Similarly, the C83A recombinant, which is probably involved in disulfide bonding and perhaps in a conformational change of the protein, was also deficient in syncytia formation. Drastic substitutions (alanine to proline) within the immunosuppressive region in mutants A60P and A64P almost completely destroyed the fusogenic capacities of the recombinant proteins. Even conservative mutations within this region (A60V, A64S, and W72L) did not permit efficient cell fusion. In contrast, mutation of the ITAM signaling motifs located within the cytoplasmic tail of gp30 recombinants Y186D, Y197D, and Y(186+197)D maintained the ability to form syncytia.

These data led us to conclude that the immunosuppressive region is required for TM protein-induced cell fusion. This functional activity of gp30 is highly susceptible to several substitutions including conservative mutations that maintain the fusogenic potential by TM proteins from other viruses (HIV-1, HTLV-I, and influenza A).

Non-conservative Mutations within the Immunosuppressive Region Destabilize the Envelope Complexes—Based on the similarities with the influenza hemagglutinin structure and theoretical considerations, our model predicts that the BLV extracellular and transmembrane envelope proteins are organized in trimeric complexes. Three gp30 molecules would interact to form the stem of the complex that would be surrounded and covered by the external gp51 glycoproteins (26). These interactions between the BLV envelope molecules appear weak since the TM protein is very easily lost during the purification of gp51 (41). For the same reason, it is not possible to analyze the oligomerization of gp51 and gp30 after centrifugation of the complexes on sucrose gradients as it has been described for other envelope proteins (42–45). However, oligomerization of BLV envelope proteins is not disrupted after centrifugation on metrizamide gradients (41). Therefore, we applied this protocol to unravel the capacity of our mutants to form oligomers. The wild-type and the different mutated envelopes were synthesized in the Semliki Forest virus expression system and applied on top of 5–40% metrizamide gradients. After centrifugation, aliquots were collected and analyzed by Western blotting using a serum from an infected sheep. Under these conditions, the wild-type (WT) envelope complexes migrate through and concentrate in the middle of the gradient (Fig. 6). Both gp30 and gp51 proteins co-localized in these fractions indicating that, indeed, metrizamide gradient centrifugation maintains the integrity of the envelope complex. In contrast, gp51 complexes with lower mobility appeared on top of the gradients after migration of the mutated envelopes (Fig. 6). The most straightforward interpretation for this observation is that the stability of the mutated envelope trimer is weakened and that the complex is separated in its different components. These low mobility complexes were particularly abundant for mutant Y197D (approximately the same amounts of low and high mobility complexes), indicating that this substitution inhibited envelope complex formation. Mutation of alanines 60 and 64 into proline residues also strongly destabilized the gp51/gp30 trimer (Fig. 6, *A60P* and *A64P*). This phenotype was expected since prolines would disturb the coiled coil structure founding the trimeric association. Even the substitution of tryptophan 72 with a leucine residue that is highly conserved among other oncoviruses (mutation W72L) interfered with envelope complex stability.

It should be mentioned here that none of the mutations completely abolished the gp30-gp51 interactions (Fig. 6). These contacts between the two envelope subunits could stabilize the latent conformation of gp30, transfer conformational changes from gp51 to gp30, or influence the interactions with the receptor. All these mechanisms could account for modifications observed in the metrizamide gradients.

Altogether, these experiments show that all the mutants exhibit, to various extends, a destabilized envelope complex formation. In particular, the envelope oligomerization was very sensitive to non-conservative mutations within the immunosuppressive region.

Mutations within the Immunosuppressive Region Affect Viral Infectivity and Proviral Loads in Vivo—Perhaps the main advantage of the BLV system is the possibility to analyze the

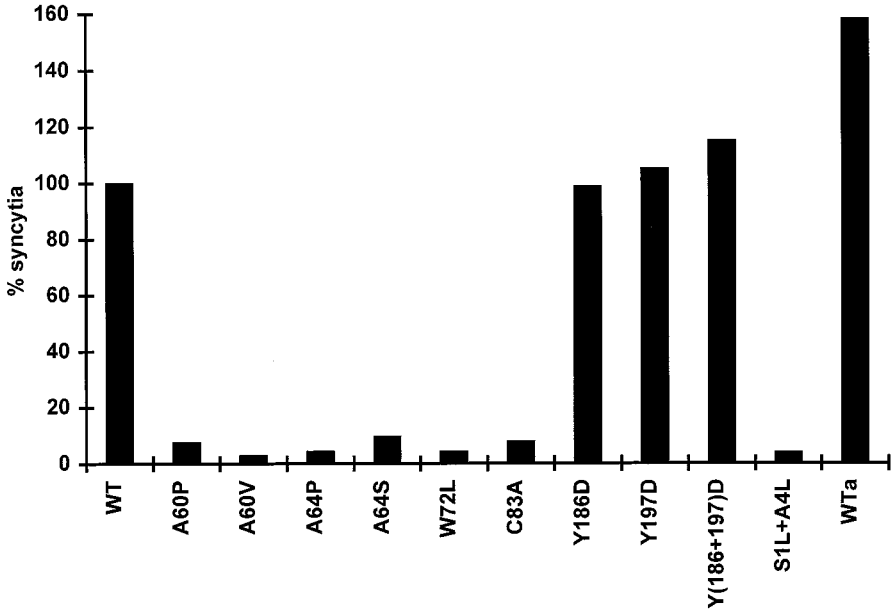

FIG. 5. **Fusogenic capacity of the recombinant BLV envelope proteins.** The fusogenic capacity of the different mutants was tested by co-cultivation of BHK cells that express the envelope proteins and CC81 indicator cells. Therefore, BHK cells were co-transfected with RNAs transcribed from pSFVLacZ (to allow visualization under the light microscope) and from the different pSFVenv vectors. After transfection, the cells were co-cultivated with CC81 indicator cells for 24 h. After fixation, the expression of *lacZ* was detected by 4-chloro-5-bromo-3-indolyl-β-galactopyranoside coloration, and the syncytia were counted in 10 different microscope fields. The numbers of syncytia are represented in percent of the wild-type level (*WT*) arbitrarily normalized to 100%. *WTa* corresponds to the American strain of a wild-type BLV virus. The data are the mean values of three independent experiments.

behavior of recombinant viruses *in vivo* (4, 13, 38, 46). The injection of sheep with BLV proviral DNA thus permits the evaluation of infectivity, viral spread, and pathogenesis as a model for the related HTLV-I virus. To assess the biological relevance of the phenotypes of the envelope mutants, a series of recombinant proviruses were constructed by using the BLV 344 strain as a template. We have indeed previously shown that this provirus 344 is infectious, propagates efficiently, and induces tumors with a mean latency period of 30 months (13, 38). As a preliminary assay, the wild-type and the 10 mutated proviruses were introduced by transient transfection into D17 canine osteosarcoma cells (as described previously in Ref. 4). The goal of this experiment was to evaluate the ability of the mutated proviruses to express viral genes in cell culture. It appeared that all the recombinant proviruses expressed equal amounts of the p24 major capsid antigen and the gp51 external envelope protein as measured by the ELISA method (39) (data not shown). The wild-type and the mutated proviruses were then injected into sheep in order to assess their infectious potential *in vivo*. Viral infectivity was evaluated by three independent methods including immunodiffusion, ELISA (see "Experimental Procedures"), and PCR (data not shown). As expected, the wild-type provirus efficiently induced the seroconversion within two animals (sheep numbers 292 and 293; Table I). Among the mutants, we have previously reported that the Y186D virus, but not the two other proviruses substituted in the cytoplasmic ITAM motifs (Y197D and Y(186+197)D was infectious *in vivo* (13). Another mutant harboring a fusion-deficient TM gene (S1L + A4L) also lost *in vivo* infectious potential. From this observation, we previously concluded that the ability to form syncytia in culture was one requirement for infectivity *in vivo* (4). Among the mutants in the immunosuppressive region, only two of them, harboring conservative mutations (A60V and A64S), were infectious after injection into sheep (numbers 492 + 493 and 500 + 228 + 107 + 108, respectively; Table I). We conclude that conservative mutations within the immunosuppressive region still allow viral infectivity *in vivo*.

To evaluate the ability of the A60V and A64S mutants to propagate efficiently within the animal, the proviral loads were measured by semi-quantitative polymerase chain reaction. Therefore, blood samples were collected by jugular venipuncture at 7 months post-seroconversion, and the corresponding viral sequences were amplified from their lysates. After 25 cycles of PCR, the amplification products were migrated on an agarose gel and hybridized with a viral probe (Fig. 7*A*). As a control for PCR contaminations, no viral product was amplified using a lysate from uninfected sheep (numbers 118 and 119). Serial dilutions of a positive control (sheep number 293) demonstrated the semi-quantitative character of the amplification. When a similar protocol was applied to lysates from sheep that are infected with provirus Y186D (276, 277, 284, and 285), it appeared that these animals harbored drastically reduced proviral loads. These data are consistent with our previous report and demonstrate that the integrity of tyrosine 186 is required for efficient viral propagation (13). An intermediate phenotype was obtained with the recombinant proviruses harboring the conservative mutations A60V and A64S. It appeared that the A64S mutant propagated at reduced levels in three animals (sheep 228, 500, and 108) (Fig. 7*A*). However, this mutant was able to propagate very efficiently in another sheep (number 107). Similarly, the proviral loads within sheep 492 and 493 that were infected with mutant A60V were close to the wild-type levels (Fig. 7*A*). To ensure that the viruses that propagated within these animals were not revertants, the envelope sequences were amplified by PCR and sequenced. As shown on Fig. 7*B*, the viruses infecting sheep 492, 493, 107, and 108 indeed harbored the expected mutations.

We conclude that the conservative substitutions in the immunosuppressive region do not destroy infectivity (as measured by immunodiffusion, ELISA, and PCR) and even maintain high levels of viral replication in some infected sheep. It thus appears that these mutants propagate efficiently despite being unable to induce syncytia in cell culture.

DISCUSSION

In contrast to the related HTLV-I system, theoretical data deduced from sequence and structure analyses from the BLV model can be correlated with experimental observations *in vivo*. In our previous studies, we have indeed learned to be cautious about the significance of *in vitro* data because it appeared that they could not always reflect the real mechanisms occurring *in vivo*. For example, the deletion of the alternative open reading frames (R3 and G4 in BLV; p12 and p30 in HTLV-I, and p10 and p28 in HTLV-II) does not affect the behavior of the provirus in cell culture even at the level of

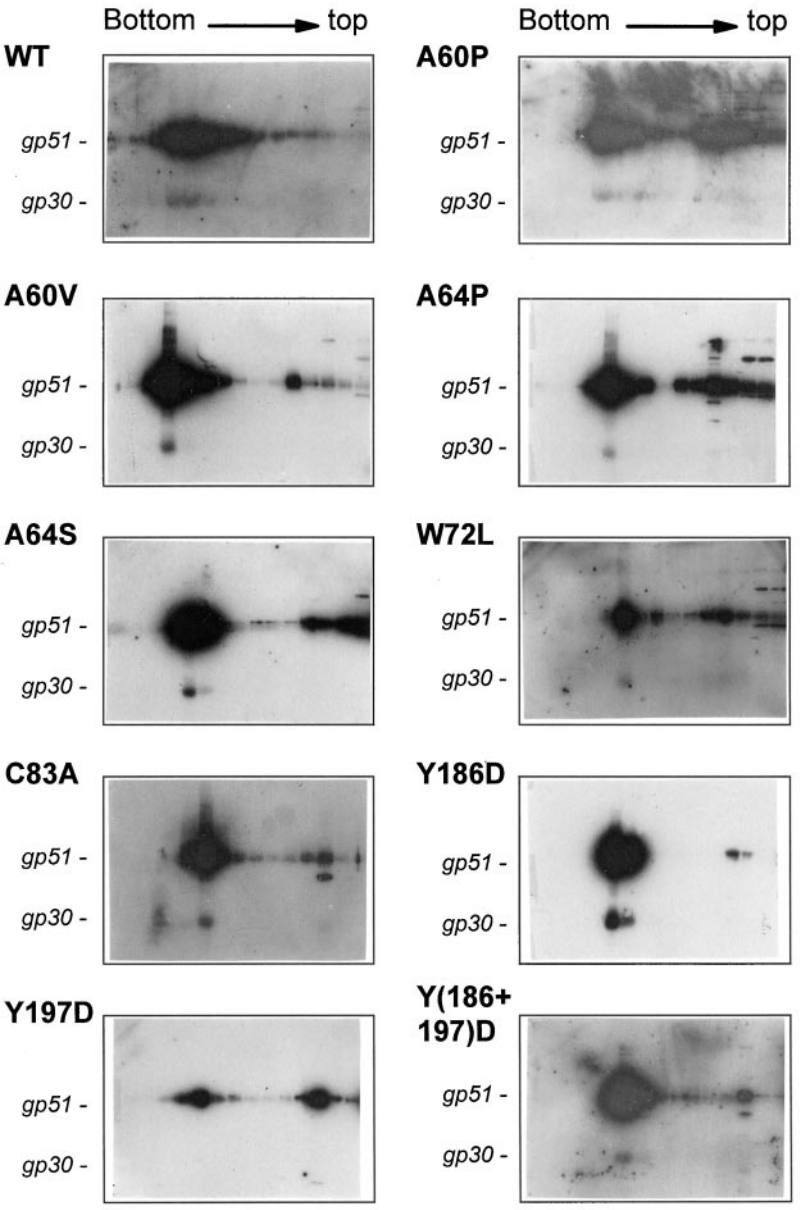

FIG. 6. **Metrizamide density gradient centrifugation of recombinant envelope glycoproteins.** The wild-type and mutated envelope genes were expressed in BHK cells. After culture, the corresponding lysates were layered onto 5–40% metrizamide gradients. After centrifugation, the fractions collected from the gradients were analyzed by Western blotting for the presence of the envelope gp30 and gp51 proteins.

immortalization of primary cells (46–48). However, the propagation of these deleted viruses is drastically reduced in the animal model demonstrating that these genes have indeed a role *in vivo* (46, 48). Therefore, the injection of sheep with recombinant proviruses still remains the best model for the analysis of similar viral-induced leukemia in humans. This strategy was applied in this report to evaluate the importance of the immunosuppressive region of the BLV TM protein that is particularly conserved among oncoviruses. By analogy with the influenza A hemagglutinin structure and on the basis of sequence analysis, the BLV TM protein can be predicted to consist in a mainly helical stem that may be reorganized in a fusion competent form by the recruitment of additional amino acids in a triple-stranded coiled coil (Fig. 1). This spring-loaded mechanism might be assumed for retroviral TM proteins although the presently known structures of retroviral TM proteins (MoMuLV and HIV-1) are limited to "fusogenic" states. Further studies of "latent" structures (in association with SU proteins) would assess such a prediction. In this model, the immunosuppressive peptide straddles both conformationally mobile regions (loop-helix B) and invariant coiled coil structures (helix C).

The goal of the present work was to correlate this theoretical model with the functional activities of the TM protein both in cell culture and *in vivo*. The survey of this report, which is summarized in Table I, reveals some expected but also surprising results. First, it is intriguing that all the mutations in the immunosuppressive region, including those that were designed to have only moderate effects, interfere with the formation of syncytia. Even substitutions by the corresponding residues of the TM proteins from other viruses such as A60V (HIV-1), A64S (influenza A HA2), and W72L (HTLV-I) did not maintain the fusogenic activity. Since none of our mutants in this region allows syncytial formation, the integrity of the BLV gp30 immunosuppressive domain thus seems essential for virus-mediated cell fusion. It thus appears that residues Ala-60, Ala-64, and Trp-72 are required for local folding of this gp30 domain. A second straightforward conclusion concerns the stability of the gp51-gp30 complex. All the substitutions interfered to various extents with the oligomerization of the envelope proteins. It was unexpected that the Y197D single mutant was unstable for oligomerization since the mutation is located in the cytoplasmic *YXXL* region. This mutant was previously reported as not infectious *in vivo*, and we hypothesized at that time that the

TABLE I
Phenotypes of the BLV gp30 mutants

Mutation names	Syncytia formation capacity[a]	Stability of gp30-gp51 complexes[b]	*In vivo* infectivity[c]	Proviral load[d]
Wild type	+	+	+	+
A60P	−	−	−	
A60V	−	±	+	+
A64P	−	−	−	
A64S	−	±	+	+/−
W72L	−	+	−	
C83A	−	±	−	
Y186D	+	±	+	−
Y197D	+	−	−	
Y(186+197)D	+	±	−	
S1L+A4L	−	ND[e]	−	

[a] The syncytia formation capacities were deduced from Fig. 5. Symbols are as follows: +, wild-type level; −, less than 10% compared with the wild-type level.

[b] The stabilities of the envelope complexes, deduced from Fig. 6, were based on the presence of low mobility complexes. + means the absence of low mobility complex, − corresponds to 50% of low mobility complexes, and ± depicts an intermediate phenotype.

[c] To assess viral infectious potential, recombinant proviruses were constructed by insertion of the mutated gp30 genes and injected into sheep. The infectious potential was evaluated by the presence of antibodies directed toward the gp51 protein (ELISA and immunodiffusion) and by PCR amplification of viral sequences.

[d] The proviral loads were estimated from the semiquantitative PCR amplifications on Fig. 7. Wild-type levels were arbitrarily set to +. For mutants A64S and Y186D, − means that the proviral loads were decreased at least 10-fold.

[e] ND, not done.

signaling pathways through the ITAM motifs are important for infectivity (13). It appears that the instability of the envelope complex could provide another direct explanation for the lack of infectious potential of this mutant. The data concerning the double mutant Y(186+197)D are more puzzling. Since this mutant but not Y197D is stable for oligomerization, we suggest that structural compensations occur between the two ITAM motifs. As expected, the introduction of proline residues within the loop at positions 60 and 64 significantly disorganized the envelope complex. The lack of correct oligomerization in mutants A60P and A64P is probably responsible for the absence of infectivity of these mutants *in vivo*. In contrast, the corresponding conservative mutations to these positions (A60V and A64S) still allowed almost WT levels of oligomerization of gp30/gp51. In addition, whereas these two mutants are unable to induce syncytia formation, they are infectious *in vivo*. How could a virus be infectious if it is unable to enter a target cell by fusion? It could be that viral infectivity and propagation occur mostly by the clonal expansion of an infected cell as it has been demonstrated in the HTLV-I system (49). In this case, the majority of the proviruses would be maintained in the infected host by a prolongation of the lifetime of their target cells. If so, other pathways of viral expansion, *i.e.* through the expression of viral particles that would subsequently colonize new lymphocytes, would only account for a minority of infected cells. It is, however, difficult to assume that this infection through viral particles is completely destroyed by the A60V and A64S mutations. In this case indeed, all the cells that harbor a recombinant virus would have been infected by the initial DNA injection, and the viral propagation would rely only on clonal expansion. Since these two routes of infection are not mutually exclusive, it is probable that viral propagation results from both clonal expansion and budding of viral particles. The other possibility is that the assay of syncytia formation lacks sensitivity because it requires high expression levels of the envelope proteins. In that respect, it has recently been shown that a decreased fusogenicity (10% of wild-type) still allows one-step viral transmission in fibroblasts transfected with HTLV-I (50).

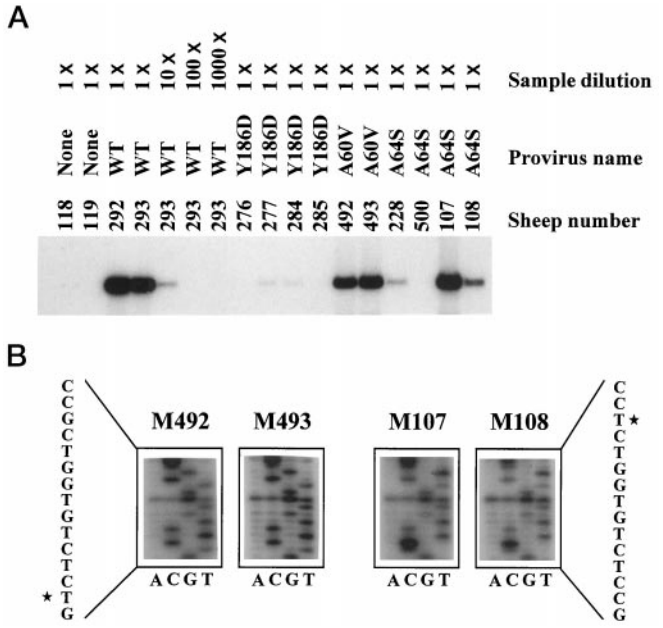

FIG. 7. **Semi-quantitative PCR amplification of proviral sequences.** *A*, DNA was extracted from 500-μl aliquots of peripheral blood and amplified by 25 cycles of PCR. The samples were then analyzed by Southern blot hybridization using a BLV Tax probe. DNAs from sheep 118, 119 (uninfected animals), 292, 293 (infected with the IX 344 provirus), and sheep 276, 277, 284, and 285 (infected with the attenuated pBLVY186D virus) were used as controls. The proviruses harboring the conservative mutations were injected into sheep 492 and 493 (for A60V) and 228, 500, 107, and 108 (for A64S) and analyzed by the same procedure. As a control for semi-quantification, serial dilutions of a positive control (sheep number 293) were amplified in parallel. *B*, direct sequencing of *in vivo* propagated viruses. The envelope genes were amplified by PCR using blood lysates from sheep 492, 493, 107, and 108. These fragments were analyzed by direct sequencing of the immunosuppressive portion of the *env* genes. The *star* delineates the position of the expected mutation.

Similarly, some membrane-fusion defective HIV mutants were still able to complement viral replication (51). In our experiments with the BLV TM mutants A60V and A64S, we have in fact observed that very few syncytia were still present in the cultures (*i.e.* less than 3% of wild-type levels). We conclude that mutants A60V and A64S that have almost completely lost their fusion ability are still infectious *in vivo* and can even propagate efficiently in some of the infected animals.

Acknowledgments—We are grateful to R. Martin, P. Ridremont, and G. Vandendaele for excellent technical help.

Addendum—After submission of this manuscript, Rosenberg and co-workers (52) demonstrated that mutations in the HTLV-I immunosuppressive region destroyed syncytium formation and reduced one-step infectivity in cell culture.

REFERENCES

1. Varmus, H. E., and Swanstrom, R. (1982) *RNA Tumor Viruses, Molecular Biology of Tumor Viruses* (Weiss, R., Teich, T., Varmus, H. E., and Coffin, J., eds) pp. 369–512, Cold Spring Harbor Laboratory, Cold Spring Harbor, NY
2. Burny, A., and Mammerickx, M. (eds) (1987) *Enzootic Bovine Leukosis and Bovine Leukemia Virus*, Martinus Nijhoff Publishing, Boston
3. Kettmann, R., Burny, A., Callebaut, I., Droogmans, L., Mammerickx, M., Willems, L., and Portetelle, D. (1994) *The Retroviridae* (Levy, J. A., ed) Vol. 3, pp. 39–81, Plenum Publishing Corp., New York
4. Willems, L., Kettmann, R., Dequiedt, F., Portetelle, D., Vonèche, V., Cornil, I., Kerkhofs, P., Burny, A., and Mammerickx, M. (1993) *J. Virol.* **67,** 4078–4085
5. Mamoun, R. Z., Morisson, M., Rebeyrotte, M., Busetta, B., Couez, D., Kettmann, R., Hospital, M., and Guillemain, B. (1990) *J. Virol.* **64,** 4180–4188
6. Vonèche, V., Portetelle, D., Kettmann, R., Willems, L., Limbach, K., Paoletti, E., Ruysschaert, J. M., Burny, A., and Brasseur, R. (1992) *Proc. Natl. Acad. Sci. U. S. A.* **89,** 3810–3814
7. Macosko, J. C., Kim, C. H., and Shin, Y. K. (1997) *J. Mol. Biol.* **267,** 1139–1148

8. Callebaut, I., Tasso, A., Brasseur, R., Burny, A., Portetelle, D., and Mornon, J. P. (1994) *J. Comput. Aided Mol. Des.* **8,** 175–191
9. Reth, M. (1989) *Nature* **338,** 383–384
10. Cambier, J. C. (1995) *Immunol. Today* **16,** 110
11. Alber, G., Kin, K. W., Weiser, P., Riesterer, C., Carsetti, R., and Reth, M. (1993) *Curr. Biol.* **3,** 333–339
12. Beaufils, P., Choquet, D., Mamoun, R. Z., and Malissen, B. (1993) *EMBO J.* **12,** 5105–5112
13. Willems, L., Gatot, J. S., Mammerickx, M., Portetelle, D., Burny, A., Kerkhofs, P., and Kettmann, R. (1995) *J. Virol.* **69,** 4137–4141
14. Cianciolo, G. J., Copeland, T. D., Oroszlan, S., and Snyderman, R. (1985) *Science* **230,** 453–455
15. Denner, J., Persin, C., Vogel, T., Haustein, D., Norley, S., and Kurth, R. (1996) *J. Acquir. Immune Defic. Syndr. Hum. Retrovirol.* **12,** 442–450
16. Ruegg, C. L., Monell, C. R., and Strand, M. (1989) *J. Virol.* **63,** 3257–3260
17. Haraguchi, S., Good, R. A., and Noorbibi, K. D. (1995) *Immunol. Today* **16,** 595–603
18. Carr, C. M., and Kim, P. S. (1993) *Cell* **73,** 823–832
19. Wilson, I. A., Skehel, J. J., and Wiley, D. C. (1981) *Nature* **289,** 366–373
20. Weis, W. I., Brunger, A. T., Skehel, J. J., and Wiley, D. C. (1990) *J. Mol. Biol.* **212,** 737–761
21. Bullough, P. A., Hugson, F. M., Skehel, J. J., and Wiley, D. C. (1994) *Nature* **371,** 37–43
22. Callebaut, I., Labesse, G., Durand, P., Poupon, A., Canard, L., Chomilier, J., Henrissat, B., and Mornon, J. P. (1997) *Cell. Mol. Life Sci.* **53,** 621–645
23. Gallaher, W. R., Ball, J. M., Garry, R. F., Griffin, M. C., and Montelaro, R. C. (1989) *AIDS Res. Hum. Retroviruses* **5,** 431–440
24. Chambers, P., Pringle, C. R., and Easton, A. J. (1990) *J. Gen. Virol.* **71,** 3075–3080
25. Delwart, E. L., Mosialos, G., and Gilmore, T. (1990) *AIDS Res. Hum. Retroviruses* **6,** 703–706
26. Callebaut, I., Portetelle, D., Burny, A., and Mornon, J. P. (1994) *Eur. J. Biochem.* **222,** 405–414
27. Fass, D., Harisson, S. C., and Kim, P. S. (1996) *Nat. Struct. Biol.* **3,** 465–469
28. Chan, D. C., Fass, D., Berger, J. M., and Kim, P. S. (1997) *Cell* **89,** 263–273
29. Weissenhorn, W., Dessen, A., Harrison, S. C., Skehel, J. J., and Wiley, D. C. (1997) *Nature* **387,** 426–430
30. Lemesle-Varloot, L., Henrissat, B., Gaboriaud, C., Bissery, V., Morgat, A., and Mornon, J. P. (1990) *Biochimie* (*Paris*) **72,** 555–574
31. Gaboriaud, C., Bissery, V., Benchetrit, T., and Mornon, J. P. (1987) *FEBS Lett.* **224,** 149–155
32. Woodcock, S., Mornon, J. P., and Henrissat, B. (1992) *Protein Eng.* **5,** 629–635
33. Cherfils, J., Vaney, M. C., Morize, I., Surcouf, E., Colloc'h, N., and Mornon, J. P. (1988) *J. Mol. Graphics* **6,** 155–160
34. Bernstein, F. C., Koetzle, T. F., Williams, G. J., Meyer, E. E., Brice, M. D., Rodgers, J. R., Kennard, O., Shimanouchi, T., and Tasumi, M. (1977) *J. Mol. Biol.* **112,** 535–542
35. Sambrook, J., Fritsch, E. F., and Maniatis, T. (1989) *Molecular Cloning: A Labolatory Manual,* 2nd Ed., pp. 1.41–1.48, Cold Spring Harbor Laboratory, Cold Spring Harbor, NY
36. Liljeström, P., and Garoff, H. (1991) *Bio/Technology* **9,** 1356–1361
37. Rice, N., Stephens, R., and Gilden, R. (1987) *Enzootic Bovine Leukosis and Bovine Leukemia Virus* (Burny, A., and Mammerickx, M., eds) pp. 115–144, Martinus Nijhoff Publishing, Boston
38. Willems, L., Portetelle, D., Kerkhofs, P., Chen, G., Burny, A., Mammerickx, M., and Kettmann, R. (1992) *Virology* **189,** 775–777
39. Portetelle, D., Mammerickx, M., and Burny, A. (1989) *J. Virol. Methods* **23,** 211–222
40. Harbury, P. B., Zhang, T., Kim, P. S., and Alber, T. (1993) *Science* **262,** 1401–1407
41. Portetelle, D., Bruck, C., Mammerickx, M., and Burny, A. (1980) *Virology* **105,** 223–233
42. Chakrabarti, S., Mizukami, T., Franchini, G., and Moss, B. (1990) *Virology* **178,** 134–142
43. Malvoisin, E., and Wild, F. (1994) *J. Gen. Virol.* **75,** 839–847
44. Poumbourios, P., el Ahmar, W., McPhee, D. A., and Kemp, B. E. (1995) *J. Virol.* **69,** 1209–1218
45. Tucker, S. P., Srinivas, R. V., and Compans, R. W. (1991) *Virology* **185,** 710–720
46. Willems, L., Kerkhofs, P., Dequiedt, F., Portetelle, D., Mammerickx, M., Burny, A., and Kettmann, R. (1994) *Proc. Natl. Acad. Sci. U. S. A.* **91,** 11532–11536
47. Green, P. L., Ross, T. M., Chen, I. S., and Pettiford, S. (1995) *J. Virol.* **69,** 387–394
48. Cockerell, G. L., Rovnak, J., Green, P. L., and Chen, I. S. (1996) *Blood* **87,** 1030–1035
49. Wattel, E., Vartanian, J. P., Pannetier, C., and Wain-Hobson, S. (1995) *J. Virol.* **69,** 2863–2868
50. Delamarre, L., Rosenberg, A., Pique, C., Pham, D., and Dokhélar, M. C. (1997) *J. Virol.* **71,** 259–266
51. Helseth, E., Kowalski, M., Gabuzda, D., Olhevsky, U., Haseltine, W., and Sodroski, J. (1990) *J. Virol.* **64,** 2416–2420
52. Rosenberg, A., Delamarre, L., Pique, C., Pham, D., and Dockelar, M. C. (1997) *J. Virol.* **71,** 7180–7186